Original Article

Influence of Manganese on the Synthesis of Nano Hydroxyapatite by Wet Chemical Method for *in vitro* Applications

Haresh M. Pandya*[1] and P. Anitha[2]

[1]Department of Physics, Chikkanna Government Arts College, Tiruppur, Tamilnadu, India
[2]P.G Department of Physics, Vellalar College for Women, Erode, Tamilnadu, India

Address for Correspondence

Department of Physics, Chikkanna Government Arts College, Tiruppur, Tamilnadu, India
E-mail: haresh.pandya@rediffmail.com

ABSTRACT

Hydroxyapatite (HAP) is an prominent biomaterial with high compatibility, bioactivity and osteoconductivity extensively employed in orthopaedics and dentistry the world over. The advantages arising from the fusion and doping of biocompatible HAP with Manganese (Mn) having excellent mechanical properties expands the horizon of biomedical applications further. The aim of the present work is to investigate the doping effect of Mn metal ions on hydroxyapatite. Pure and Mn doped HAP with various four different concentrations were prepared by wet chemical method. The final samples were characterized for phase composition via XRD, functional analysis through FTIR, surface morphological analysis via SEM and elemental analysis by EDAX. The synthesis powders were characterized by X-ray diffraction (XRD), Fourier Transform infrared spectroscopy (FTIR), scanning electron microscopy (SEM) and energy dispersive X - ray spectra (EDAX).

Keywords: Hydroxyapatite, Biocompatibility, Manganese, XRD, SEM, FTIR.

INTRODUCTION

Hydroxyapatite (HAP) is a mineral from the family of apatite. The general formula of which is $M_5(ZO_4)_3X$ where M is a rare earth metal such as Ca^{2+}, Cd^{2+}, Sr^{2+}, Ba^{2+}, Pb^{2+}, Zn^{2+} or Mg^{2+}. ZO_4 could be PO_4^{3-}, CO_3^{2-}, or SO_4^{2-} and X is OH^-, F^-, Cl^- or CO_3^{2-}, whereas $Ca_5(PO_4)_3OH$ is the formula for HAP, $Ca_{10}(PO_4)_6(OH)_2$ is the formula of the unit cell. HAP is therefore the most stable calcium orthophosphate phase in the pH range of 4.2 to 12.4[1].

HAP bio ceramics are frequently employed basic materials in bone implant surgery. Due to such features, as high biocompatibility, bioactivity and very good adaptation under *in vivo* conditions[2] they are widely applied to fill bone defects in orthopedics, maxillofacial surgery as well as stomatology and dentistry. However, one of the most important disadvantages of HAP biomaterials is their brittleness and low load bearing mechanical property which

precludes them from getting employed in applications that require high mechanical loads[3,4]. Thus development of biocompatible HAP with enhanced mechanical properties is very much desirable and welcome in the above mentioned areas of its application[5]. The load bearing disadvantage is usually rectified by synthesizing HAP through hot processing and hot isostatic processing techniques. An alternative economical technique to obtain highly dense HAP body at low temperature is by incorporating additives or dopants during powder processing[6-8].

One of the main reasons for adding Mn^{2+} ion as additives in hydroxyapatite bulk material is that, its density is enhanced without any phase transformation even if the material is sintered or calcined at 1300C[9]. Further, Mn^{2+} ions have increased potential for ligand binding affinities to integrins and thus assist as well as trigger faster cell adhesion and osteoblast bonding[10-14]. Further, as the radius of Mn^{2+} ion(0.80Å) is closer to that of Ca^{2+} ion(1.0 Å), Mn^{2+} ions can easily substitute Ca^{2+} ions in either hydroxyapatite or beta tri calcium phosphate.

Synthesis of Nano phase HAP compounds have been resorted to in the present study because they demonstrate improved biocompatibility when compared to bulk HAP.[15] Moreover, since Mn ions get oxidized at higher values of pH, in the present study, the pH values of Mn dopant solution have been restricted between 5.8-6.0[16,17].

Thus the aim of the present work is to investigate the role of Manganese in the growth of hydroxyapatite nano particles and its effect on changes in crystal size and crystallinity of hydroxyapatite during its synthesis

There are various well established procedures for the synthesis of nano powders[18,19] of hydroxyapatite such as - continuous precipitation from solution[20], hydrothermal processing[21], electro spraying[22], electro spinning[23], flux cooling method[24], spray pyrolysis[25], microwave irradiation[26], wet chemical synthesis based on hydrolysis of metal organic precursors and chemical vapor[27] and plasma deposition[28].

The Wet Chemical Method of synthesis has been adopted in the present study for its excellent control of size, shape, crystallinity, homogeneous and high degree of purity of nano HAP as well as of the low capital costs.

SAMPLE PREPARATION PROCEDURE

The chemicals for synthesis of Mn doped hydroxyapatite include calcium hydroxide ($Ca(OH)_2$), ortho phosphoric acid (H_3PO_4), Manganese chloride tetra hydrate ($MnCl_2.4H_2O$) and ammonia which were purchased and used without further purification.

Pure $Ca_{10-x}Mn_x(PO_4)_6(OH)_2$ with x=0 was synthesised with Ca/P mole ratio 1.67 using wet chemical method. 1M of calcium hydroxide and 0.6M of Orthophosphoric acid were prepared separately and the designated amount of Ortho phosphoric acid was dissolved in calcium hydroxide to form 1.67 mole/L solutions. The mixture was stirred for 2hrs using magnetic stirrer. The pH was constantly monitored and adjusted at 10 during the reaction using ammonia. After reaction, the deposited mixtures were washed several times with deionised water. The resulting material was dried at 100^0C in electrical air oven.

$$10Ca(OH)_2+6H_3PO_4 \longrightarrow Ca_{10}(PO_4)_6(OH)_2 + 18H_2O$$

Manganese doped hydroxyapatite $Ca_{10-x}Mn_x(PO_4)_6(OH)_2$ with x=0.1, 0.2, 0.5, 1 Wt% was prepared by setting the ratio Ca+Mn/P as 1.67. The $MnCl_2.4H_2O$ and

$Ca(OH)_2$ were dissolved in deionized water to obtain 100ml [Ca+Mn] containing solution. The [Ca+Mn] containing solution was stirred for 30 minutes. The Orthophosphoric acid solution was added to [Ca+Mn] solution drop wise and stirred for 1 hr. The pH of the solution was adjusted and kept at 5.6 during the reaction. After the reaction, the deposited mixture was washed several times with deionized water. The prepared powders with various Mn concentrations were dried at 100C using electrical air oven.

MATERIAL CHARACTERIZATION

X-ray Diffraction [XRD]

Phase analysis of pure HAP and MnHAP powders was conducted using XRD using Cu K-α radiation (λ=1.5418Å) equipped with Silicon detector at a range of angles 10^o to 70^o with 60 second exposures. Crystallographic identification of the MnHAP was accomplished by comparing the experimental pattern to the standard complied by JCPDS: HAP card No #09 – 0432. The size of individual MnHAP crystallite was calculated from XRD data using the Debye's Scherer equation given below, and the peak of (001) and (300) were fit to define its full width half maximum intensity.

$$d = K\lambda / \beta_{1/2} \cos\theta$$

Where, d is the crystallite size as calculated for the hkl reflection, λ is the wavelength of Cu K- α radiation and K is the broadening constant varying with crystal lattice and chosen as 0.9 for the elongated apatite crystallite, θ is the angle of diffraction and β is the full width half maximum intensity.

Possible changes in the crystal structure (lattice parameters) were quantified. Interplanar distance (d value) obtained by XRD (peak 25 – 27^o = 002 planes: peak 30 – 35^o = 211 and 300 planes; peak 39 – 40^o = 310 planes) allowed the calculation of the parameters 'a' and 'c' from the crystal lattice following the equation

$$\lambda = 2d_{hkl}\sin\theta_{hkl}$$

$$1/d^2_{hkl} = 4/3[h^2 + hk + l^2]a^2 + l^2/c^2$$

Fourier Transform Infrared Spectroscopy [FTIR]

In order to examine the functional groups present in pure and Mn doped HAP, FTIR was performed to study the powder in the range of wavelength 4000 – $400cm^{-1}$ using typical KBr pellet technique.

Scanning Electron Microscopy [SEM]

The structure and morphology of the prepared powder samples was studied using SEM. For detailed elemental analysis, the electron microscope was equipped with an energy dispersive X- ray attachment (EDAX).

RESULTS AND DISCUSSION

Crystallite Size & Lattice Parameters

X-ray diffraction pattern of the synthesized HAP powders was well in agreement with the JCPDS data for stoichiometric HAP. No other phase such as β – TCP, octacalcium phosphate, calcium oxide and toxic material were detected in the sample. The replacement of calcium ions by manganese atoms generates a small change in the peak values indicating the influence of Mn doping as evident in Figure 1 which shows XRD graph for pure and doped hydroxyapatite.

For an undoped hydroxyapatite, the crystallite size calculated from Debye's Scherer formula is 20nm. For a Mn doped HAP with various concentrations, the crystallite size ranges from 24nm to 70 nm.

This is due to the presence of Mn concentration.

The XRD of HAP and MnHAP also demonstrated that powders made by wet chemical at 100C exhibit the apatite characteristics with good crystal structure and no new phase or impurities was found. The addition of Mn however, induces a distinct color change of nano HAP from white to brown. The intensity of the brown colour increases with increase in the Mn concentration.

As evident from Table 1, crystallite size and lattice parameters for Mn HAP nano powders decreases with increase in Mn concentration. This result is expected as calcium is progressively substituted by metal ions during the mineralization process.

Functional Groups

Figure 2 shows the FTIR spectra of pure and Mn doped HAP. FTIR spectroscopy was performed to investigate the functional groups in hydroxyapatite with various concentrations at 100C by wet chemical method. These data mainly reveal the presence of the various vibrational modes corresponding to phosphate and hydroxyl groups. For all the samples, presence of strong OH^{-1} vibration peak is noted. The broad bands in the region 1600 – 1700cm^{-1} and 2500 – 3900cm^{-1} correspond to H-O-H bonds of lattice water. The larger bands are attributed to adsorbed water which get diminished at higher concentrations. These changes can be attributed to the substitution of Ca by Mn in the lattice of apatite. Bands corresponding to phosphate groups in apatite were observed at 1097, 1058, 962, 565, 472cm^{-1} for PO_4^{3-} groups.

Extra Complementary information can be obtained from spectra. The vibrational bands at 472cm^{-1} is attributed to the O-P-O bending modes. The bands present at 1058cm^{-1} can be assigned to asymmetric P-O stretching. The frequency 603 and 565cm^{-1} can be addressed mainly to O-P-O bending characters.

Bands observed in the FTIR spectrum are characteristics of crystallized apatite phase similar to the apatite phase observed in XRD patterns.

Surface Morphology

The morphology of the nano particle of HAP and Mn HAP was investigated by SEM. SEM image provide the direct information about the typical shape and width of the as prepared samples. The SEM image and EDAX spectrum of Mn HAP with x = 0 to 1.5wt% are shown in Figures 3, 4 and 5. The results suggest that the doping Mn has little influence on the morphology of HAP. The spectra and the image confirms the presence of Mn on HAP. The EDAX spectrum of Mn HAP confirms the presence of calcium [Ca], Phosphor [P], Oxygen [O] and Manganese [Mn] in the sample. The SEM image also showed the formation of nano rod like structures with the width of about 40 – 60nm in all the samples.

CONCLUSION

In this study, Mn doped HAP has been synthesised by wet chemical method. the results of the experimental work can be summarized as follows:

- XRD studies reveals that characteristic peaks of HAP in each are present and the crystallite size increases with increase in the concentration of Mn material.
- The addition of Mn has an influence in the structural and morphological behavior of Mn doped HAP.
- EDAX studies confirmed the presence of elements and SEM studies results in the formation of nano rods in all the samples.
- In agreement with the XRD and SEM, FTIR studies show that the absorption characteristics of HAP and OH groups

decreased with increase in the Mn concentration

The Present study also shows that the prepared Mn doped HAP is more biocompatible due to its being nano rod like in structure.

REFERENCES

1. Vuk Uskokovic, Dragon P Uskokovic. Nanosized hydroxyapatite and other calcium phosphate chemistry formation and application as drug and gene delivery agents. *Wiley Online library*. 2010.
2. P.Anitha, Haresh M Pandya. Synthesis, Characterization and Antimicrobial activity of Nano hydroxyapatite via a novel Sol Gel method. *Nano technology Research and Practice*. 2014; 3(3); 120-126.
3. Sanash K P, Min Cheol Chu, Balakrishnan A, Yong Jim Lee, Seong Jai Cho. Synthesis of nano hydroxyapatite powder that simulate teeth particle morphology and composition. *Current Applied Physics*. 2009,;9; 1459-1460.
4. Ducheyne P, Groot K.de. In vivo surface activity of a hydroxyapatite alveolar bone substitute. *Journal of Biomedical Material Res*. 1981;15; 442- 445.
5. Ramesh S, Tan C Y, Peralta C L, Teng W S. The effect of Manganese Oxide on the sinterability of hydroxyapatite. *Science and Technology of Advanced materials*. 2007;,8 ;257-262.
6. P.Anitha, Haresh M. Pandya. Synthesis, Characterization and Invitro evaluation of Titanium Doped nano hydroxyapatite by novel wet chemical method. *Journal of International Academic Research for Multidisciplinary*. 2014; 2(8); 374-378.
7. Wojciech Suchanek, Masatomo Yashima, Masato Kakihana, Masahiro Yoshimura. Hydroxyapatite Ceramics with Selected Sintering additives. *Biomaterials,* 1997, 18(13), 923-933.
8. Li Zy, Lam WM, yang C, Xu B, Ni GX, Addah SA, Cheung KM. Chemical composition Crystal size and lattice structureal changes after incorporation of Strontium into biomimetric apatit. *Biomaterials*. 2007; 26;1452-1460.
9. Yan Li, jasmine Widodo, Sierin Lim. Synthesis and Cytocompatibility of Manganese and Iron substituted hydroxyapatite nanoparticle. *Journal of Material Science*.2011.
10. Czeslava palszkrewicz, Anna Slosccyk, Dawid Pijocha. Syntheis structural properties and thermal stability of Mn doped hydroxyapatite. *Journal of molecular structure*.2010;976; 301-309.
11. Sopyan I, Nawawi NA, Shan QH, Ramesh S. Sintering and properties of Manganese doped Calcium Phosphate Bioceramics prepared by sol gel derived nanopowders. *Materials and Manufacturing processes*. 2011;,26; 908-914.
12. Mayer I, Cuisinier FJG, Popor J Schleich. Phase relation between beta tricalcium phosphate and hydroxyapatite with Manganese Ii: structure and spectroscopic properties. *European Journal of Chemictry*, 2006;7 ;1460-1465.
13. Kazuhiko K, Hironobu S, Tamoyoki y. Local environment analysis of Mn ions into beta tricalcium phosphate. *Journal of Japan ceramic society*. 2008;16(116); 108-110.
14. Yan Li, Jasmin Widodo, Sierin Lim. Synthesis and Cyto Compatibility of Manganese and iron substituted hydroxyapatite nanoparticle. *Journal of Material Science.* 2011.
15. Mayer I, Jacobsohn O, Niazor T, Werchmann J, Iliesar M, Richard Ploute M. *European Journal of Inorganic Chemistry*, 2003; 1445.
16. Wedsite T, Ergun C, Doremur RH, Siegal R W, Bizios R. Enhanced functions of Osteoblasts on nanophase Ceramics. *Biomaterials*, 2000; 21(17);1803-1810.
17. Haresh M. Pandya. Modelling Scenario in nanotechnology Today. *Journal of Environmental Nano technology*, 2012;1(1); 01-04.
18. P.Anitha, Haresh M. Pandya. Comprehensive review of preparation methodologies of nano hydroxyapatite. *Journal of Environmental nano technology*. 2013;3(1); 101-121.
19. Gomez Morales J, Torrent Burgues J, Boix T, Fraile J. Precipitation of Stoichiometric hydroxyapatite by a continuous method. *Crystal Res Technol*.2001;36; 15-25.
20. Ashok M, Kalkura SN, Sundaram NM, Arivoli D. Growth and characterization of

hydroxyapatite crystals by hydrothermal method. *Journal of Material Science, Material medicine*. 2007; 18;895-898.
21. Hian ES Ahmad Z, Huang J, Edirisingha MJ, Jayasinghe SN, Ireland DC, Brooks RA. The role of surface wettability and surface charge of electrosprayed nanoapatites on the behaviour of osteoblasts. *Acta Biomaterial*. 2010;6(3);750-755.
22. Hae- Wan kim, Hyoun Ee Kim. Nanofiber generation of hydroxyapatite and flour hydroxyapatite bioceramics. *Wiley Interscience*, 2005; Nov 8.
23. Cuneyt Tas A. Molten Salt Synthesis of Calcium hydroxide whiskers. *Journal of Chemical Ceramic Society*. 2001; 84(2); 295-300.
24. Vukoman Jokanovic ,Dragon Uskokovic. Calcium hydroxyapatite thin film on titanium substrate prepared by ultrasonic spray pyrolysis. *Materials Transaction*. 2005; 46(2); 228 -235.
25. Erdem Hasret, Mehmet Ipekoglu, Sabri Altintas. Microwave assisted synthesis of hydroxyapatite for the removal of lead(II) from aqueous solution. Environmental Science and Pollution Research2011;19(7); 2766-2775.
26. Naruporn monmaturapoj. Nanosized hydroxyapatite powders preparation by wet chemical precipitation route. *Journal of Metals, Material and Minerals*. 2008;1;115-20.
27. Hao Wang, Noam Eliaz, Zhou Xiang, Larly. Bone opposition in vivo on plasma sprayed and electro chemical deposited hydroxyapatite coating on titanium alloy. *Biomaterials,*.2006;27;4192- 4201.
28. N.rameshbabu, T.S Sampath kumar, T.G. Prabakar, V.S.Sadtry. Antibacterial nano sized silver substituted hydroxyapatite; Syntheisi and Characterization. *Journal of Bio materials Research part A*.2007;80(3); 581-591.

Table 1: XRD Calculations for pure and Mn HAP formation

Sample	Crystallite Size in nm	Lattice Parameter		Unit Cell Volume in 10^{-30} m^3
		a in Å	c in Å	
Pure HAP	29	9.378	6.8124	1551.14
MnHAP1	70	9.4843	6.9270	1613.198
MnHAP2	30	9.4507	6.8744	1589.625
1MnHAP3	25	9.4396	6.8588	1582.294
MnHAP4	24	9.4277	6.8124	1567.304

ISSN 2321 – 2748

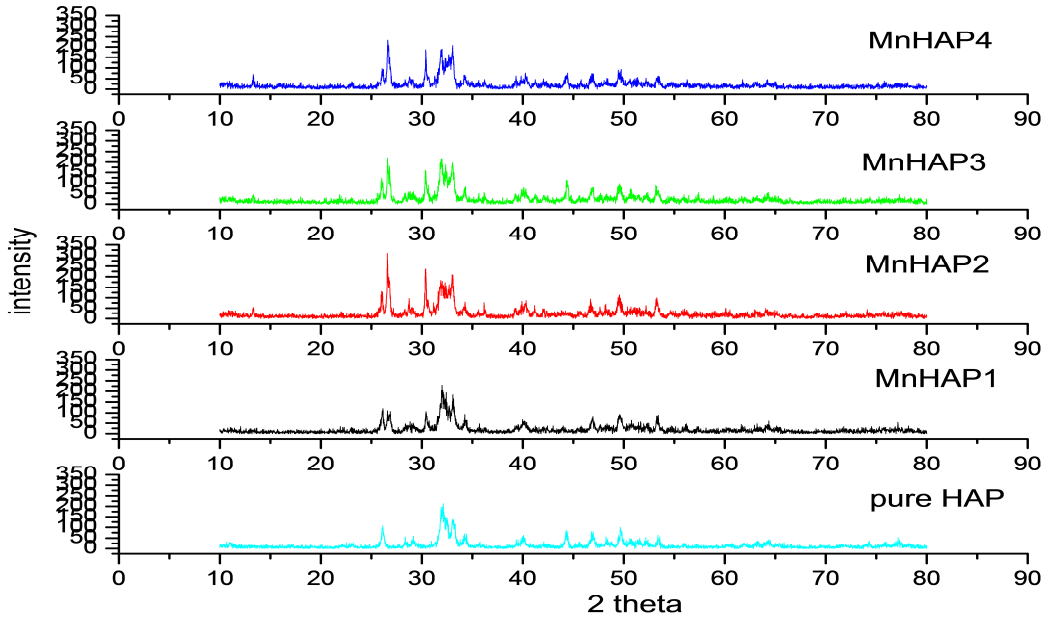

Fig. 1: XRD spectra of pure and Mn doped HAP.

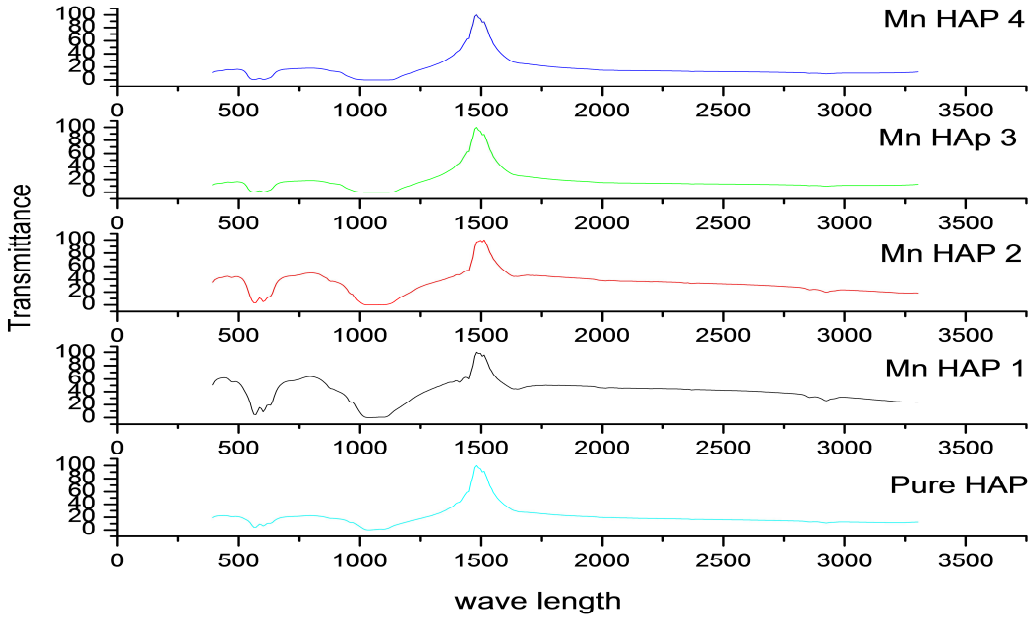

Fig. 2: FTIR spectra of pure and Mn doped HAP.

 ISSN 2321 – 2748

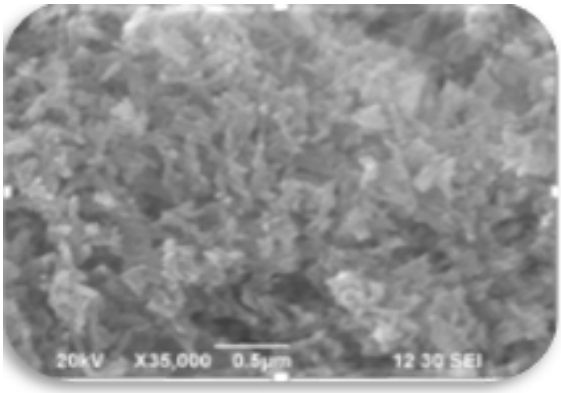

Fig. 3: SEM image of Pure nano HAP

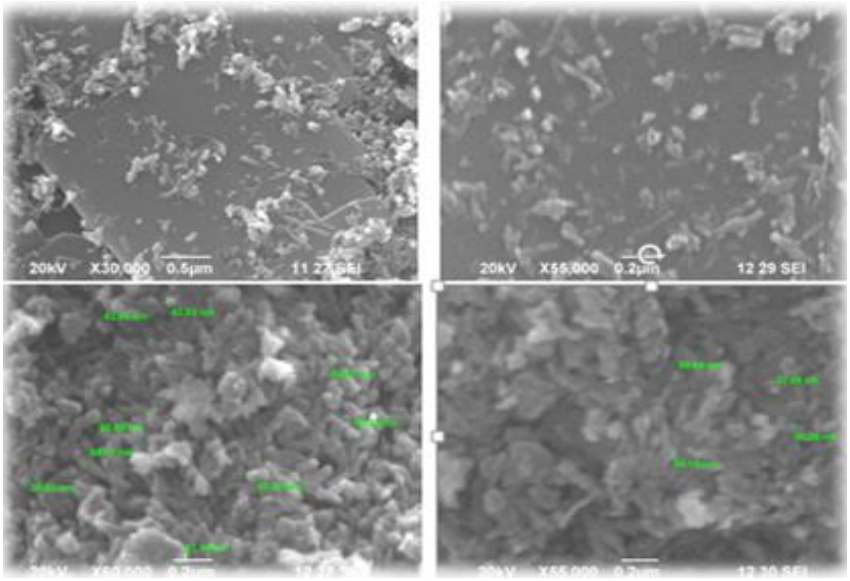

Fig. 4: SEM images of MnHAP at various Concentrations.

 ISSN 2321 – 2748

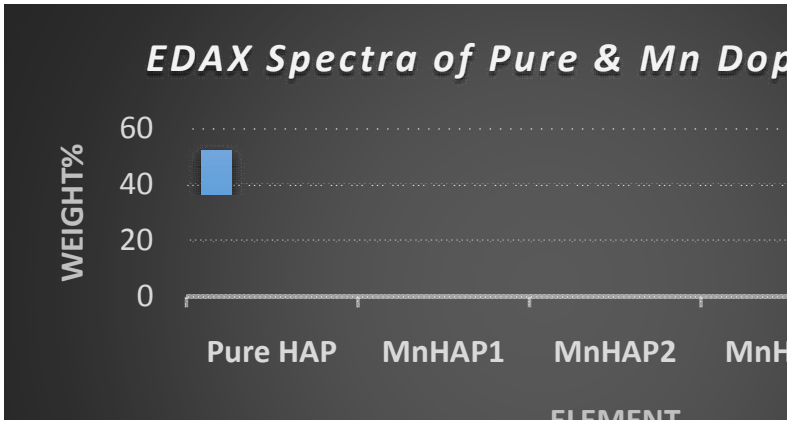

Fig. 5: SEM images of MnHAP at various Concentrations.